eLife

Reviewed Preprint
v1 • September 9, 2025
Not revised

Reviewed Preprint
v2 • July 22, 2026
Revised by authors

For correspondence:
l.m.veenhoff@rug.nl

Competing interests: No competing interests declared

Funding: See page 11

Reviewing editor: Elçin Ünal, University of California, Berkeley, United States

A tool to pulse-label yeast Nuclear Pore Complexes in imaging and biochemical experiments

Annemiek C Veldsink[1], Jonas S Fischer[2], Sophie Hell[2], Karsten Weis[2], Liesbeth M Veenhoff[1]

[1]European Research Institute for the Biology of Ageing, University of Groningen, University Medical Center Groningen, Groningen, Netherlands • [2]Institute of Biochemistry, Department of Biology, ETH Zurich, Zurich, Switzerland

eLife Assessment

This **important** study introduces a non-perturbative pulse-labeling strategy for yeast nuclear pore complexes (NPCs), employing a nanobody-based approach in order to selectively capture Nup84-containing complexes for imaging and biochemical analysis. The data **convincingly** demonstrate that a short induction period (20 minutes to 1 hour) yields a strong and sustained signal, enabling affinity purification that faithfully recapitulates the endogenous Nup84 interactome. This tool offers a powerful framework for investigating NPC dynamics and associated interactomes through both imaging and biochemical assays.

https://doi.org/10.7554/eLife.108399.2.sa4

Abstract

Nuclear Pore Complexes (NPCs) are key gateways to the nucleus and major organizers of genome architecture. Despite their importance, it is still not fully understood how NPCs are formed and degraded. Tools to track specific NPCs over time or under stress could unlock critical insights into these questions. Here, we demonstrate that a brief pulse of expression of a previously developed nanobody against baker's yeast nucleoporin Nup84 (Nordeen et al. 2020) enables a robust, rapid, and straightforward method for pulse-labeling NPCs in both imaging and affinity purification experiments. This approach offers an alternative to permanent yet less rapid genetic fluorophore- or tag-switching techniques and provides a powerful tool for studying NPC inheritance and turnover through both microscopy and biochemical methods.

Rapid labeling of NPCs using a nanobody against Nup84

Single domain antibodies, nanobodies, have been developed and used for structural biology (Nordeen et al. 2020), for protein purifications (Stankunas and Köhler 2024) and for probing *in vivo* protein assemblies (Solà Colom et al. 2024). A previously developed nanobody (VHH) against the yeast nucleoporin (Nup) Nup84 (Nordeen et al. 2020), a conserved member of the outer ring structures of NPCs, binds Nup84 with nanomolar affinity (VHH-SAN8, from here on VHH[Nup84]) (Nordeen et al. 2020). According to recent structures of the yeast NPC (Singh et al. 2024; Nordeen et al. 2020), the Nup84 epitope is peripherally located in the fully assembled structure, facing both the cytoplasm and nucleoplasm and thus providing an accessible site for nanobody pulse-labeling. To examine the use of VHH[Nup84] as a tool to fluorescently pulse-label NPCs, we fused it to mNeongreen (mNG), a bright fluorophore with short maturation times in yeast (Guerra et al. 2022). We placed the construct under an inducible galactose promoter, allowing for time-controlled expression bursts (Figure 1A), albeit with some cell-to-cell and experimental variability in expression level. Expression of VHH[Nup84]-mNG did not affect cell

viability or growth rates, as also previously shown (Nordeen et al. 2020). We observed colocalization of VHH[Nup84]-mNG with NPCs marked by the endogenously tagged NPC component Pom34-mCh (Figure 1B) and no detectable NE signal was observed in nup84Δ cells (Figure 1C), confirming previous structural studies showing that VHH[Nup84] specifically binds Nup84 (Nordeen et al. 2020). Noteworthy, a short, 20-minute expression burst was enough to give a detectable NE signal until at least two hours after the initial induction (Figure 1B, D). Quantifying the signal, we measure that in the first two hours after a 20-minute expression pulse, the mean intensity of VHH[Nup84] reached approximately 46% +/- 27% of the intensity of endogenously tagged Nup84 (Figure 1E). A longer, 1hr-induction pulse further increased the labeling of NPCs compared to a 20-minute expression pulse and the fluorescence levels become indistinguishable (108% +/- 33%) from those obtained with endogenously tagged Nup84 (Figure 1D, E, Figure 1 – supplement 1). Given that the NE labeling intensities are ultimately determined by both incorporation of new VHH[Nup84]-mNG into NPCs as well as the dilution of labeled NPCs to daughter cells, it makes sense that the maximal labeling intensities measured follow the division times in minimal medium (+/- 2hr) (Figure 1E). Collectively, these findings show that pulse-labeling Nup84 in NPCs is quick and tunable, providing an alternative to endogenous tagging of NPC subunits.

VHH[Nup84]-ZZ is a suitable bait for NPC affinity purifications

In addition to the use of VHH[Nup84]-mNG as a pulse-labeling tool in imaging experiments, we characterized the value of VHH[Nup84] as a bait in affinity purifications (APs) of NPCs. We tagged VHH[Nup84] with a tandem Z domain (ZZ-tag), a protein A derived tag that can be purified using IgG-coated beads. We constitutively expressed VHH[Nup84] from the Nup120 promoter and found that all nucleoporins (Nups), except Pom33 and Gle1, significantly coenriched with VHH[Nup84]-ZZ as compared to control APs in cells expressing a free ZZ-tag (Figure 1G, Source data Figure 1). Importantly, the level to which Nups are enriched is comparable to APs with endogenously tagged Nup84-ZZ (Figure 1F) and overall, there is a strong correlation between APs using the VHH[Nup84]-ZZ and the Nup84-ZZ baits (R2 = 0.91) (Figure 1H). This demonstrates that VHH[Nup84] can be used as an affinity bait to purify NPCs, on par with endogenously tagged Nup84-ZZ.

Next, we set out to investigate the affinity purification efficiency of VHH[Nup84]-ZZ when used to pulse-label NPCs. We used a short, 20-minute induction burst to express the VHH[Nup84]-ZZ bait and subsequently determined its interactome at various timepoints (Figure 1I). This short expression pulse was enough to specifically purify NPCs 1.5 hours after the induction (Figure 1I) and we could already confidently identify most Nups 10 minutes after the start of bait expression. Their intensity increased at the 30 min timepoint and did not drastically change 1.5 hours after labeling start (Figure 1I). This indicates that pulse-labeling is very fast and that VHH[Nup84]-ZZ stays stably bound to the NPC over longer times. Hence, VHH[Nup84]-ZZ can be a powerful tool to pulse-label NPCs to assess the interactome of NPCs at specific points in time.

VHH[Nup84] can be used to trace labeled NPCs in time

Considering that exchange of individual Nups, including Nup84, is generally slow with half times in the order of hours (Hakhverdyan et al. 2021; Rabut, Doye, and Ellenberg 2004), and that the nanobody:Nup84 association is very stable (Nordeen et al. 2020), we wondered whether we could use VHH[Nup84] pulse-labeling to follow labeled NPCs over longer time periods. Using the same experimental set-up described in Figure 1A, we imaged cells 4hrs and 8hrs after the short 20 min induction pulse. At 8hrs, the signal was diluted from NE rings (Figure 1B, D) to individual foci (Figure 1J), indeed indicating the inheritance of labeled NPCs to daughter cells in mitosis. To quantify the number of foci per cell, we employed the PunctaFinder plugin that can detect foci in

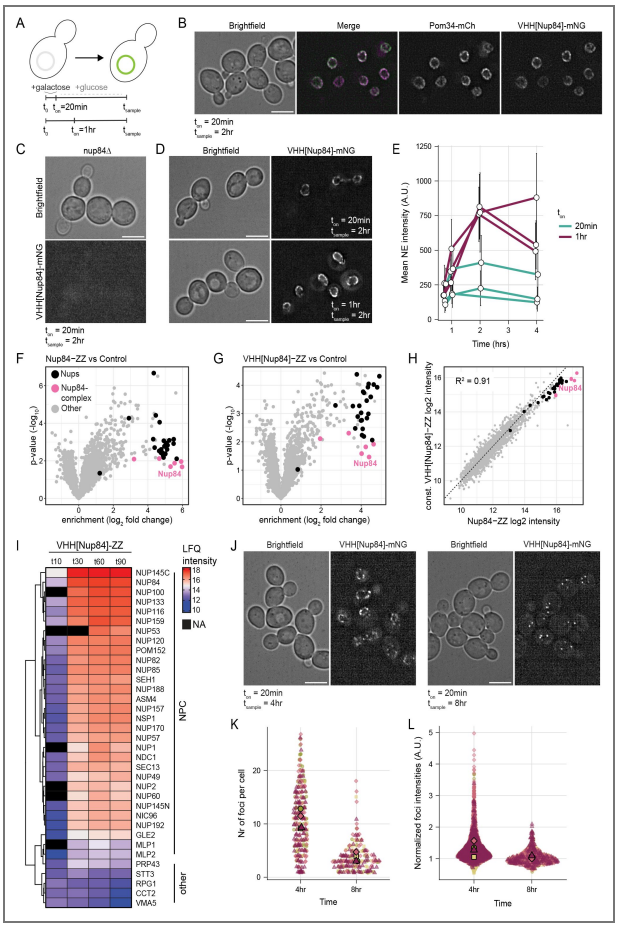

Figure 1. Nanobody against Nup84 is a tool to pulse-label yeast NPCs in imaging and biochemical experiments

A) Schematic of the experimental set-up. At t_0, VHH[Nup84]-mNG is expressed for the specified amount of time (t_{on}) by addition of 0.5% galactose to the medium. Expression is subsequently shut off by addition of 1% glucose and images are taken at time (t_{sample}) to determine NPC labeling. **B)** Colocalization of VHH[Nup84]-mNG with Pom34-mCh at t=2hr following a 20min induction pulse. Images represent summed projections of 3 z-slices (midplane +/- 0.5 µm). Scale bar = 5 µm. **C)** Typical image of VHH[Nup84]-mNG in nup84Δ cells at t=2hr following a 20min induction pulse. Images represent a single z-slice. Scale bar = 5 µm **D)** Typical images of VHH[Nup84]-mNG at t=2hr following either a 20min or 1hr induction pulse. Images represent sum projections of 3 z-slices (midplane +/- 0.1 µm). Scale bar = 5 µm. **E)** Quantification of NE intensities in the midplane of cells at various timepoints following a 20min (cyan) or 1hr (purple) induction pulse. Data represents mean NE intensity +/- standard deviation of three biological replicas. Numbers of cells analyzed (ton - t_{sample}): 102 (20min-45min), 139 (20min-1hr), 82 (20min-2hr, *N=2*), 92 (20min-4hr), 111 (1hr-45min), 186 (1hr-1hr), 153 (1hr-2hr), 193 (1hr-4hr). Mean NE intensity +/- standard deviation of endogenously tagged Nup84-mNG is 726 +/-148 (224 cells). **F)** Volcano plot showing the log2 fold enrichment of proteins in affinity purifications using endogenously expressed Nup84-ZZ as a bait compared to mock-ZZ. Nups are colored in black, the Nup84 subcomplex is colored in magenta. **G)** Volcano plot showing the log2 fold enrichment of proteins in affinity purifications using VHH[Nup84]- ZZ constitutively expressed from the Nup120 promoter as a bait compared to mock-ZZ. Nups are colored in black, the Nup84 subcomplex is colored in magenta. **H)** Correlation between protein intensities in the affinity purifications with VHH[Nup84] from **F** and **G**. **I)** Heat map showing log2 intensities of Nups and five randomly selected non-enriched proteins ("Other") in VHH[Nup84]-ZZ affinity purifications at the various sampling timepoints following a 20 min VHH[Nup84] induction pulse. LFQ = label free quantitation. **J)** Typical image of the localization of VHH[Nup84]-mNG at t=4hr and t=8hr following a 20-minute induction pulse. Each panel represents a sum projection of 5 consecutive z-slices (0.1 µm). Scale bar = 5 µm. **K)** Quantification of the number of VHH[Nup84]-mNG foci per cell at t=4hr and t=8hr following a 20-minute induction pulse. Each dot represents a cell, each color reflects a biological replica. Means per replica are indicated. Nr of cells analyzed (t_{on} - t_{sample}): 289 (20min-4hr), 215 (20min-8hr) from four biological replicas. **L)** Intensities of detected VHH[Nup84]-mNG foci at t=4hr and t=8hr following a 20-minute induction pulse. Intensities are normalized to median foci intensity at t=8hr of the corresponding replica. Each dot represents a single focus, each color reflects a biological replica. Means per replica are indicated. Nr of cells analyzed (t_{on} - t_{sample}): 289 (20 min-4 hr), 215 (20min-8hr) from four biological replicas. See Figure 1–Source Data 1 for source data to EFGHIKL.

3D (Terpstra et al. 2024). Between 4 and 8hrs, the median number of foci per cell decreased from 11 to 3 (Figure 1K), which is consistent with cell cycle kinetics and a previous reports showing that approximately 40% of the existing NPCs are transmitted to the daughter cell in each division (Zsok et al. 2024; Khmelinskii et al. 2010). The spread in foci intensities decreased in time (Figure 1L), which is likely related to the high density of >10 NPC/µm2 NE (Winey et al. 1997) that compromises the detection of individual pores when they are all labeled. The median intensity reduced by approximately 20% between 4 and 8hrs (Figure 1L), consistent with the stable association of VHH[Nup84] with NPCs. Considering that the rapid labeling of NPCs leads to a quick depletion of unbound VHH[Nup84]-mNG from the cytosol, these foci very likely reflect NPCs that were labeled in the early time stages. Thus, VHH[Nup84]-mNG allows the visualization and tracking of individual NPC over time.

Altogether, we show that VHH[Nup84] is a tool for pulse-labeling of NPCs in live yeast cells in imaging and biochemical experiments. The pulse-labeling of Nup84 in NPCs with VHH[Nup84]-mNG is quick and tunable, providing an alternative to endogenous tagging of NPC subunits. Amongst others this is useful in conditions where direct tagging of Nup84 interferes with its function, while sub stoichiometric nanobody binding may not, or when the temporary introduction of a ZZ- or mNG-tagged nanobody allows assessment of the integrity or localization of mutant NPCs prior to performing experiments without the nanobody. The rapid binding of VHH[Nup84]-mNG to NPCs is stable and hence allows the imaging of individual NPCs in time over multiple divisions. Pulsed expression of VHH[Nup84] thus provides an alternative to the recombination-induced tag exchange (RITE) cassette or optically switchable fluorophores (Verzijlbergen et al. 2010; Zsok et al. 2024; Toyama et al. 2019; Colombi et al. 2013; Zhou and Lin 2013; Onischenko et al. 2020). Lastly, ZZ-tagged VHH[Nup84] can be used as an affinity bait to purify NPCs, on par with endogenously tagged Nup84-ZZ, and, when expressed shortly it can be used to assess the interactome of NPCs at specific points in time or under specific conditions. While our pulse-labeling strategy uses an inducible galactose promoter, other inducible promoters that do not require carbon-source shifts, such as the Gal4-ER-VP16 system (Louvion, Havaux-Copf, and Picard 1993), could be beneficial in conditions when alterations in the metabolic state of the cell are disadvantageous.

As NPCs are long-lived structures, VHH[Nup84] may specifically allow for NPC inheritance studies or the characterization of aged NPCs that were labeled early on during the experiment. Along the same line, we envision that applying genetic perturbations or environmental stresses such as oxidizing conditions, heat stress or osmotic shock at the time of VHH[Nup84] pulse-labeling, provides a means to study the long-term fate of these NPCs. For example, this could resolve the question whether these NPCs are specifically degraded. Similarly, we envision that VHH[Nup84] pulse-labeling strategies can also be used to inducibly bring specific proteins in proximity of NPC, e.g. for determining the local and time resolved interactome of NPCs using proximity labeling strategies (Filali-Mouncef et al. 2024). These and other future studies tracking NPC inheritance and studying NPC turnover mechanisms might uncover how the quality of NPCs is maintained and how this fails in ageing and disease.

Methods

Yeast strains and growth

All strains used in this study are listed in the key resources table. Strains were generated using standard microbiology techniques and validated by microscopy and/or PCR. For all pulse-labeling experiments, strains were inoculated 2 days prior to the experiment and grown in synthetic minimal medium supplemented with 2% D-glucose (30°C, 200rpm). On day -1, cells were diluted in minimal medium supplemented with 2% D-raffinose and grown to exponential phase, maintaining them in mid-exponential phase from this point onwards. At the start of the experiment, VHH[Nup84] expression was induced by addition of 0.5% galactose to the medium (2% in the affinity purification experiment; panel I), followed by addition of 1% glucose (2% in the affinity purification experiment; panel I) after 20 minutes or 1hr as described in the figure.

Reagent type (species) or resource	Designation	Source or reference	Identifiers	Additional information
Saccharomyces cerevisiae	W303 *MATa leu2-3,112 trp1-1 can1-100 ura3-1 ade2-1 his3-11,15*	Open biosystems		
S. cerevisiae	yAV108 W303 *leu2::pGAL1-VHH[Nup84]-mNeongreen::LEU2*	This study	yAV108	VHH[Nup84]-mNG under galactose promoter integrated in the leu2 locus using pAV49
S. cerevisiae	yAV115 W303 *leu2::pGAL1-VHH[Nup84]-mNeongreen::LEU2 POM34-mCherry::URA3*	This study	yAV115	C-terminal tagging of POM34-mCherry using pPP014 (Rempel et al. 2019)
S. cerevisiae	yAV173 W303 *NUP84-mNeongreen::URA3*	This study	yAV173	C-terminal tagging of NUP84-mNeongreen using pAV54 (Otto et al. 2024)
S. cerevisiae	yAV178 W303 *leu2::pGAL1-VHH[Nup84]-mNeongreen::LEU2 nup84Δ::Hyg*	This study	yAV178	Deletion of nup84 using pFA6-HphNT1
S. cerevisiae	yAV213 W303 *lys2Δ::KanMX, leu2::pGAL1-VHH[Nup84]-S-TEV-ZZ::HIS3,LEU2*	This study	yAV213	VHH[Nup84]-S-TEV-ZZ under galactose promoter integrated in the leu2 locus with HIS3 selection marker, using pKW803 to replace mNG with S-TEV-ZZ. Lys2 deletion by PCR amplification of lys2 deletion cassette from YKO collection
S. cerevisiae	KWY12171 W303 *lys2Δ::KanMX his3::pNUP120-VHH[Nup84]-S-TEV-ZZ::HIS3*	This study	KWY12171	Constitutively expressed VHH[Nup84]-S-TEV-ZZ in the his3 locus
S. cerevisiae	KWY12149 W303 *lys2Δ::KanMX NUP84-S-TEV-ZZ::HIS3*	(Onischenko et al. 2020)	KWY12149	
recombinant DNA reagent	pRS305 (plasmid)	Addgene (Markus, Punch, and Lee 2009)	pRS305	Integrative vector with LEU2 marker
recombinant DNA reagent	pPP014 (plasmid)	(Rempel et al. 2019)	pPP014	PCR template for C-terminal mCherry tagging; URA3 selection
recombinant DNA reagent	pFA6-HphNT1 (plasmid)	(Janke et al. 2004)	pFA6-HphNT1	Gene deletion cassette; hygromycin resistance
recombinant DNA reagent	pKW803 (plasmid)	(Onischenko et al. 2020)	pKW803	

Key resources table.

recombinant DNA reagent	pAV49 (plasmid)	This study	pAV49	*pGAL1-VHH[Nup84]-mNeongreen-Cyc in pRS305 backbone*
recombinant DNA reagent	pAV54 (plasmid)	(Otto et al. 2024)	pAV54	*PCR template for C-terminal mNeongreen tagging; URA3 selection*
chemical compound, drug	D-Glucose anhydrous	Fisher	G/0500/65	
chemical compound, drug	D(+)-Raffinose pentahydrate	Thermo Scientific	195675000	
chemical compound, drug	D-Galactose	Acros Organics	150610010	
chemical compound, drug	Minimal medium	Sigma Aldrich		
chemical compound, drug	Protease inhibitor cocktail	Sigma-Aldrich	P8215	
chemical compound, drug	Dynabeads M-270 Epoxy	Invitrogen	14301	
chemical compound, drug	Purified IgG protein from rabbit serum	Sigma-Aldrich	I5006	
chemical compound, drug	Coomassie Brilliant Blue R-250	Bio-Rad	161-0400	
chemical compound, drug	Sequencing grade porcine trypsin	Promega	V5113	
chemical compound, drug	L-Lysine:2HCL (13C6, 99%; 15N2, 99%)	Cambridge Isotope Laboratories	CNLM-291-H-0.25	
chemical compound, drug	Iodoacetamide	Sigma-Aldrich	I1149	
chemical compound, drug	Ammonium bicarbonate	Sigma-Aldrich	9832	
chemical compound, drug	Formic acid 99–100%	VWR Chemicals	20318.297	
chemical compound, drug	iRT Kit	Biognosis	Ki-3002-1	
chemical compound, drug	BioPureSPN MINI Columns Silica C18	The Nest Group, Inc	HUM S18V	
chemical compound, drug	BioPureSPN MACRO Columns Silica C18	The Nest Group, Inc	HMM S18V	
software, algorithm	ImageJ/FIJI	(Schindelin et al. 2012)		

Key resources table. (continued)

software, algorithm	PunctaFinder	(Terpstra et al. 2024)		
software, algorithm	R version 4.1.0	(RCoreTeam; 2024)		
software, algorithm	Rstudio v. 26.01.1	Posit Software, PBC		
software, algorithm	SoftWoRx	Cytiva		
software, algorithm	Illustrator v. 30.2.1	Adobe		
software, algorithm	Jupyter Notebook v. 6.5.4	Project Jupyter		
software, algorithm	Python v. 3.11.4	Python Software Foundation		
other	screw-cap micro tubes	Sarstedt Inc.	72.693.005	
other	mini-BeadBeater-24, 230 Volt	BioSpec Products	112011EUR	

Key resources table. (continued)

Fluorescence microscopy

Images were acquired using a Deltavision Elite (Applied Precision) microscope, using an Olympus UPlanSApo 100x (NA 1.4) oil immersion objective and equipped with an EDGE sCMOS5.5 camera for detection. Images were acquired in 30 Z-slices of 0.1 µm, except for panel B (3 z-slices of 0.5 µm). SoftWoRx software (GE Healthcare) was used for image deconvolution and images were processed using Fiji software (ImageJ 2.14.0) (Schindelin et al. 2012). NE intensities were measured in Fiji by drawing line scans over the NE in the midplane and correcting for background intensity. Dumbbell shaped NEs or cells without visible NE staining were excluded from analysis, as were cells in which line scans could not be confidently drawn.

Affinity purifications and proteomic data acquisition and analysis

Proteomic experiments and data analysis were essentially performed as described in (Kralt et al 2022). To induce expression of VHH bait, cells were grown to mid-log phase as described above and then transferred from medium containing 2% raffinose to medium containing 2% galactose. After 20 minutes of induction, bait expression was halted by directly adding 2% glucose (v/v). At the specified timepoints, samples equivalent to 250 mL of culture of OD600 of 1 were harvested by filtration and snap-frozen in liquid nitrogen. For metabolic labelling experiments, cells were transferred from light L-lysine medium (25 mg/L) containing 2% raffinose to heavy, 13C6 15N2 L-lysine (Cambridge Isotope Laboratories) medium containing 2% galactose to concomitantly start VHH expression and metabolic labelling.

All steps of the affinity purification protocol were performed on ice, minimizing delays to maintain protein complex integrity. Frozen yeast pellets were resuspended in lysis buffer (20 mM HEPES pH 7.5, 50 mM KOAc, 20 mM NaCl, 2 mM MgCl2, 1 mM DTT, 10% v/v glycerol) and transferred to 2 mL screwcap microtubes (Sarstedt Inc.) pre-filled with ~1 mL of 0.5 mm glass beads (BioSpec Products). The tubes were topped up with additional lysis buffer, and cells were lysed mechanically using a Mini BeadBeater-24 (BioSpec Products) in four 1-minute cycles at 3500 oscillations per minute, with 1-minute cooling intervals in ice water between cycles. Cell debris and unlysed cells were pelleted at 850 x g for 30 s at 4°C and 1 mL of the resulting supernatant was supplemented with 110 µL 10× detergent mix (protease inhibitor cocktail [Sigma-Aldrich], 5% v/v Triton x-100, 1% v/v Tween-20 in lysis buffer). This mixture was transferred to a fresh tube with 1 mg IgG-coated pre-equilibrated magnetic beads (Invitrogen Dynabeads M-270 Epoxy #14301; Sigma rabbit IgG serum #I5006). Samples were incubated at 4°C for 30 minutes with continuous mixing. Beads weore then washed four times with 1 mL of wash buffer (0.1% v/v Tween-20 in lysis buffer) and bound proteins were eluted in 40 µL of 1× Laemmli sample buffer for 2 minutes at 50°C. Eluates were then denatured at 95°C for 5 minutes.

Proteins were concentrated by SDS-PAGE using a 4% acrylamide stacking gel, then incubated in distilled water for 12 hours to remove residual detergents. Protein bands were excised and processed using a standard in-gel digestion protocol. In brief, disulfide bonds were reduced with dithiothreitol (6.5 mM DTT in 100 mM ammonium bicarbonate) for 1 hour at 60°C, followed by alkylation with iodoacetamide (54 mM in 100 mM ammonium bicarbonate) for 30 minutes at 30°C in the dark. Proteins were then digested with 1.25 µg trypsin (Promega) in 100 mM ammonium bicarbonate for 16 h at 37°C. Peptides were desalted using C18 BioPureSPN mini columns (The Nest Group, Inc), washed with Buffer A (0.1% v/v formic acid), eluted with Buffer B (0.1% v/v formic acid, 80% v/v acetonitrile), and ultimately recovered in 12.5 µL Buffer A supplemented with iRT peptides (1:50 v/v, Biognosys).

LC-MS/MS analysis was performed on an Orbitrap Exploris 480 mass spectrometer (Thermo Scientific) coupled to a Vanquish Neo UHPLC system (Thermo Scientific). Peptide separation was achieved on a C18 reversed-phase column (75 µm x 400 mm (New Objective), packed in-house with ReproSil Gold 120 C18, 1.9 µm (Dr. Maisch GmbH)). For the time course samples with the inducible VHH[Nup84] construct, peptides were eluted using a 120-minute linear gradient from 7% to 35% buffer B (0.1% [v/v] formic acid, 80% [v/v] acetonitrile) at a flow rate of 300 nl/min. The mass spectrometer was operated in data-independent acquisition (DIA) mode using one MS1 scan (350-

1150 m/z, 120000 resolution, 250% normalized AGC target, 264 ms maximum injection time), followed by 41 variable MS2 windows from 350-1150 m/z with 1 m/z overlap (30000 resolution, 250% normalized AGC target, 64 ms maximum injection time). Fragmentation was carried out by HCD at normalized collision energy (NCD) 28%. For constitutively expressed VHH[Nup84] samples, a 60-minute non-linear gradient from 1% to 43.7% buffer B at a flow rate of 300 nl/min was used. DIA was performed with one MS1 scan (330-1650 m/z, 120000 resolution, 300% normalized AGC target, 20 ms maximum injection time), followed by 30 variable MS2 windows from 330 to 1650 m/z with 1 m/z overlap (30000 resolution, 2000% normalized AGC target, 64 ms maximum injection time). Fragmentation was also performed using HCD, with NCE set to 27%.

The data from the time course samples were extracted with Spectronaut v18.2 (Biognosys) using a spectral library previously generated from 60 APs with 11 Nup baits (Kralt et al. 2022). Data from constitutively expressed VHH[Nup84] were extracted with Spectronaut v19.1 using the directDIA workflow. Carbamidomethylation was used as fixed modification and methionine oxidation, and N-terminal acetylation were set as variable modifications. Tryptic peptides with less than two missed cleavages were considered, and spectra were searched against the *Saccharomyces cerevisiae* protein database (downloaded from SGD on 13/10/2015, 6713 entries). For DIA data analysis in Spectronaut, all default settings were kept except that “cross-run normalization” was turned off. The ion intensities at the fragment level were exported and analysed in R as follows: first, low-quality precursors were excluded based on Spectronaut’s “F. ExcludedFromQuantification” flag. All remaining fragment ions with an intensity > 4 were summed. Only prototypic precursors were retained and precursor intensities were summarized into protein intensities using the MaxLFQ method (Cox et al. 2014). Proteins with less than two identified precursor ions in all three replicates of one timepoint were filtered out. Protein intensities were median normalized per sample, and the mean of three biological replicates was used as the final protein intensity. Statistical significance was assessed using a two-tailed Student’s t-test. The samples with inducible VHH[Nup84] were originally acquired using SILAC with isotopically labelled lysine. However, for our analysis, we relied on label-free quantification by summing the ion intensities of heavy and light y-type fragment ions from precursors containing a single lysine. To account for missing values, pairwise dissimilarities in Fig 1I were computed using the daisy algorithm from the cluster package in R, which accommodates NA values by using all available variable pairs. For comparison, 5 non-NPC proteins were randomly chosen from the list of all reproducibly co-purified proteins. See Figure1-Source Data for LFQ intensities, fold-enrichment, and statistics for all detected proteins.

PunctaFinder analysis

PunctaFinder analysis (Terpstra et al. 2024) (panels K, L) was essentially performed as described in (Veldsink et al. 2025), using the same threshold settings (Tlocal = 1.478 (ratio punctum/surroundings) and Tglobal = 1.816 (ratio punctum/cell)). Subsequent filtering steps were omitted as the absence of cytosolic VHH[Nup84]-mNG pools did not require additional filtering of detected puncta. Output was analyzed using R software version 4.1.0 (RCoreTeam; 2024). For median normalization of foci intensities (panel L), intensities of all foci at t=4hrs and t=8hrs were divided by the median foci intensity at t=8hr of the same replica.

Graphs and statistics

Graphs and statistical analysis were performed using R software version 4.1.0 (RCoreTeam; 2024). Data in panels K, L was plotted according to the SuperPlot guidelines (Lord et al. 2020).

Supplementary figures

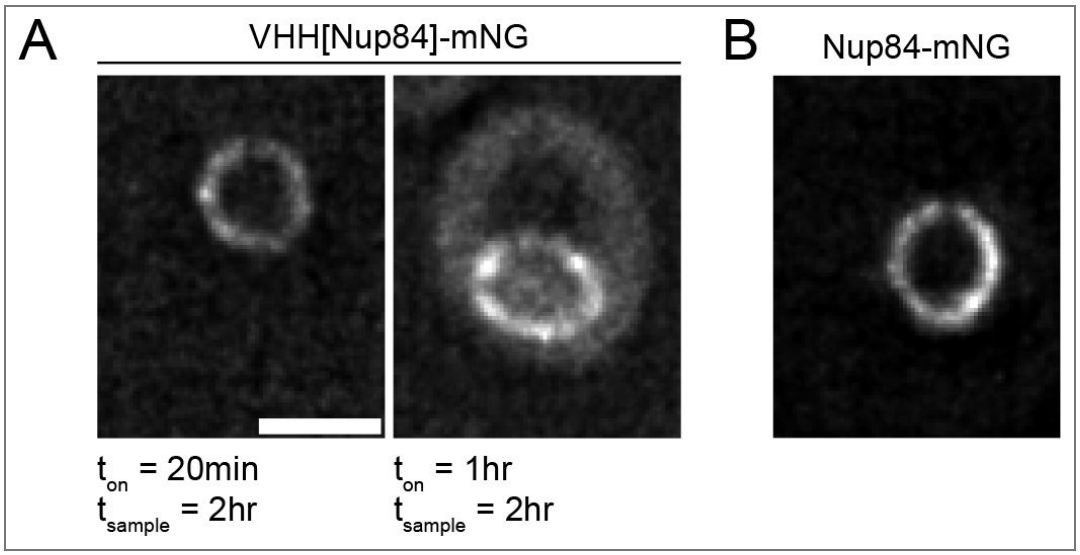

Figure 1 - supplement 1. Typical images of a cell expressing VHH[Nup84]-mNG (A) or endogenously tagged Nup84-mNG (B). VHH[Nup84]-mNG expressing cells were imaged at t=2hr following either a 20min (left) or 1hr induction pulse (right). Images represent sum projections of 3 z-slices (midplane +/- 0.1 µm). Scale bar = 2 µm

Data availability

Source data files have been provided for all figures.

Acknowledgements

We kindly thank Prof. Dr. Thomas Schwartz (MIT) for sharing the Nup84 nanobody. We thank Federico Uliana and Ino D Karemaker from the IBC MS facility. We thank Michael Chang all members of the Chang and Veenhoff labs for valuable input. Annemiek Veldsink was supported by a PhD-fellowships from the Graduate School of Medical Sciences of the University of Groningen. This work was supported by a Vici grant (VI.C.192.031) to LMV from the Netherlands Organisation for Scientific Research and funding to KW from the Swiss National Science Foundation (TMAG-3_209354 CRSII5_193740).

Additional information

Author contribution

Conceptualization: ACV, JSF, KW, LMV; Investigation: ACV, JSF, SH; Methodology, formal analysis, data curation, visualization: ACV, JSF; Writing—original draft —review & editing: ACV, JSF, KW, LMV; Supervision and funding acquisition: ACV, KW, LMV.

Impact statement

a non-perturbative nanobody-based strategy for pulse-labeling yeast nuclear pore complexes (NPCs) to selectively capture Nup84-containing complexes for imaging and biochemical analysis.

Funding

Funder	Grant reference number	Author
Nederlandse Organisatie voor Wetenschappelijk Onderzoek (NWO)	VI.C.192.031	Liesbeth M Veenhoff
Schweizerischer Nationalfonds zur Förderung der Wissenschaftlichen Forschung (SNF)	TMAG-3_209354 CRSII5_193740	Karsten Weis

Author ORCID iDs

Karsten Weis: https://orcid.org/0000-0001-7224-925X
Liesbeth M Veenhoff: https://orcid.org/0000-0002-0158-4728

Additional files

Figure 1–Source Data 1.

References

Colombi Paolo, Webster Brant M, Fröhlich Florian, Lusk C Patrick (2013) The transmission of nuclear pore complexes to daughter cells requires a cytoplasmic pool of Nsp1. *Journal of Cell Biology* **203**:215-32 https://doi.org/10.1083/jcb.201305115 | PubMed

Cox J, Hein MY, Luber CA, Paron I, Nagaraj N, Mann M (2014) Accurate proteome-wide label-free quantification by delayed normalization and maximal peptide ratio extraction, termed MaxLFQ. *Mol Cell Proteomics* **13**:2513-26 https://doi.org/10.1074/mcp.m113.031591 | PubMed

Filali-Mouncef Y, Leytens A, Duarte P Vargas, Zampieri M, Dengjel J, Reggiori F (2024) An APEX2-based proximity-dependent biotinylation assay with temporal specificity to study protein interactions during autophagy in the yeast Saccharomyces cerevisiae. *Autophagy* **20**:2323-37 https://doi.org/10.1080/15548627.2024.2366749 | PubMed

Guerra Paolo, Vuillemenot Luc-Alban, Rae Brady, Ladyhina Valeriia, Milias-Argeitis Andreas (2022) Systematic In Vivo Characterization of Fluorescent Protein Maturation in Budding Yeast. *ACS Synthetic Biology* **11**:1129-41 https://doi.org/10.1021/acssynbio.1c00387 | PubMed

Hakhverdyan Z, Molloy KR, Keegan S, Herricks T, Lepore DM, Munson M, Subbotin RI, Fenyo D, Aitchison JD, Fernandez-Martinez J, *et al.* (2021) Dissecting the Structural Dynamics of the Nuclear Pore Complex. *Mol Cell* **81**:153-65 e7 https://doi.org/10.1016/j.molcel.2020.11.032 | PubMed

Janke C, Magiera MM, Rathfelder N, Taxis C, Reber S, Maekawa H, Moreno-Borchart A, Doenges G, Schwob E, Schiebel E, *et al.* (2004) A versatile toolbox for PCR-based tagging of yeast genes: new fluorescent proteins, more markers and promoter substitution cassettes. *Yeast* **21**:947-62 https://doi.org/10.1002/yea.1142 | PubMed

Khmelinskii Anton, Keller Philipp J, Lorenz Holger, Schiebel Elmar, Knop Michael (2010) Segregation of yeast nuclear pores. *Nature* **466**:E1-E1 https://doi.org/10.1038/nature09255 | PubMed

Kralt A, Wojtynek M, Fischer JS, Agote-Aran A, Mancini R, Dultz E, Noor E, Uliana F, Tatarek-Nossol M, Antonin W, *et al.* (2022) An amphipathic helix in Brl1 is required for nuclear pore complex biogenesis in S. cerevisiae. *eLife* **11** https://doi.org/10.7554/elife.78385 | PubMed

Lord Samuel J, Velle Katrina B, Mullins R Dyche, Fritz-Laylin Lillian K (2020) SuperPlots: Communicating reproducibility and variability in cell biology. *Journal of Cell Biology* **219** https://doi.org/10.1083/jcb.202001064 | PubMed

Jean-François Louvion, Havaux-Copf Biserka, Picard Didier (1993) Fusion of GAL4-VP16 to a steroid-binding domain provides a tool for gratuitous induction of galactose-responsive genes in yeast. *Gene* **131**:129-34 https://doi.org/10.1016/0378-1119(93)90681-r | PubMed

Markus SM, Punch JJ, Lee WL (2009) Motor- and tail-dependent targeting of dynein to microtubule plus ends and the cell cortex. *Curr Biol* **19**:196-205 https://doi.org/10.1016/j.cub.2008.12.047 | PubMed

Nordeen SA, Andersen KR, Knockenhauer KE, Ingram JR, Ploegh HL, Schwartz TU (2020) A nanobody suite for yeast scaffold nucleoporins provides details of the nuclear pore complex structure. *Nat Commun* **11**:6179 https://doi.org/10.1038/s41467-020-19884-6 | PubMed

Onischenko E, Noor E, Fischer JS, Gillet L, Wojtynek M, Vallotton P, Weis K (2020) Maturation Kinetics of a Multiprotein Complex Revealed by Metabolic Labeling. *Cell* **183**:1785-800.e26 https://doi.org/10.1016/j.cell.2020.11.001 | PubMed

Otto TA, Bergsma T, Dekker M, Mouton SN, Gallardo P, Wolters JC, Steen A, Onck PR, Veenhoff LM (2024) Nucleoporin Nsp1 surveils the phase state of FG-Nups. *Cell Rep* **43**:114793 https://doi.org/10.1016/j.celrep.2024.114793 | PubMed

Gwénaël Rabut, Doye Valérie, Ellenberg Jan (2004) Mapping the dynamic organization of the nuclear pore complex inside single living cells. *Nature Cell Biology* **6**:1114-21 https://doi.org/10.1038/ncb1184 | PubMed

RCoreTeam (2024) R: A Language and Environment for Statistical Computing.

Rempel Irina L, Crane Matthew M, Thaller David J, Mishra Ankur, Jansen Daniel PM, Janssens Georges, Popken Petra, Akşit Arman, Kaeberlein Matt, van der Giessen Erik, *et al.* (2019) Age-dependent deterioration of nuclear pore assembly in mitotic cells decreases transport dynamics. *eLife* **8**:1-26 https://doi.org/10.7554/elife.48186 | PubMed

Schindelin Johannes, Arganda-Carreras Ignacio, Frise Erwin, Kaynig Verena, Longair Mark, Pietzsch Tobias, Preibisch Stephan, Rueden Curtis, Saalfeld Stephan, Schmid Benjamin, *et al.* (2012) Fiji: an open-source platform for biological-image analysis. *Nature Methods* **9**:676-82 https://doi.org/10.1038/nmeth.2019 | PubMed

Singh D, Soni N, Hutchings J, Echeverria I, Shaikh F, Duquette M, Suslov S, Li Z, van Eeuwen T, Molloy K, *et al.* (2024) The molecular architecture of the nuclear basket. *Cell* **187**:5267-81.e13 https://doi.org/10.1016/j.cell.2024.07.020 | PubMed

Solà Colom M, Fu Z, Gunkel P, Güttler T, Trakhanov S, Srinivasan V, Gregor K, Pleiner T, Görlich D (2024) A checkpoint function for Nup98 in nuclear pore formation suggested by novel inhibitory nanobodies. *EMBO J* **43**:2198-232 https://doi.org/10.1038/s44318-024-00081-w | PubMed

Stankunas E, Köhler A (2024) Docking a flexible basket onto the core of the nuclear pore complex. *Nat Cell Biol* **26**:1504-19 https://doi.org/10.1038/s41556-024-01484-x | PubMed

Terpstra HM, Gómez-Sánchez R, Veldsink AC, Otto TA, Veenhoff LM, Heinemann M (2024) PunctaFinder: An algorithm for automated spot detection in fluorescence microscopy images. *Mol Biol Cell* **35**:mr9 https://doi.org/10.1091/mbc.e24-06-0254 | PubMed

Toyama Brandon H, Drigo Rafael Arrojoe, Lev-Ram Varda, Ramachandra Ranjan, Deerinck Tomas J, Lechene Claude, Ellisman Mark H, Hetzer Martin W (2019) Visualization of long-lived proteins reveals age mosaicism within nuclei of postmitotic cells. *Journal of Cell Biology* **218**:433-44 https://doi.org/10.1083/jcb.201809123 | PubMed

Veldsink Annemiek C, Fischer Jonas S, Terpstra Hanna M, Mannino Philip, de Lange Eline MF, Hell Sophie, van Benthem Koen J, Saba Leila J, Steen Anton, Vlijm Rifka, *et al.* (2025) Detecting Nuclear Pore Complex assembly in living cells. *BioRxiv* https://doi.org/10.1101/2025.07.30.667432

Verzijlbergen KF, Menendez-Benito V, van Welsem T, van Deventer SJ, Lindstrom DL, Ovaa H, Neefjes J, Gottschling DE, van Leeuwen F (2010) Recombination-induced tag exchange to track old and new proteins. *Proc Natl Acad Sci U S A* **107**:64-8 https://doi.org/10.1073/pnas.0911164107 | PubMed

Winey M, Yarar D, Giddings TH, Mastronarde DN (1997) Nuclear pore complex number and distribution throughout the Saccharomyces cerevisiae cell cycle by three-dimensional reconstruction from electron micrographs of nuclear envelopes. *Mol Biol Cell* **8**:2119-32 https://doi.org/10.1091/mbc.8.11.2119 | PubMed

Zhou XX, Lin MZ (2013) Photoswitchable fluorescent proteins: ten years of colorful chemistry and exciting applications. *Curr Opin Chem Biol* **17**:682-90 https://doi.org/10.1016/j.cbpa.2013.05.031 | PubMed

Zsok J, Simon F, Bayrak G, Isaki L, Kerff N, Kicheva Y, Wolstenholme A, Weiss LE, Dultz E (2024) Nuclear basket proteins regulate the distribution and mobility of nuclear pore complexes in budding yeast. *Mol Biol Cell* **35**:ar143 https://doi.org/10.1091/mbc.e24-08-0371 | PubMed

Peer reviews

Reviewer #1 (Public review):

Summary:

The authors present a nanobody-based pulse-labeling system to track yeast NPCs. Transient expression of a nanobody targeting Nup84 (fused to NeonGreen or an affinity tag) permits selective visualization and biochemical capture of NPCs. Short induction effectively labels NPCs, and the resulting purifications match those from conventional Nup84 tagging. Crucially, when induction is repressed, dilution of the labeled pool through successive cell cycles allows the visualization of "old" NPCs (and potentially individual NPCs) providing a powerful view of NPC lifespan and turnover without permanently modifying a core scaffold protein.

Strengths:

(1) A brief expression pulse labels NPCs, and subsequent repression allows dilution-based tracking of older (and possibly single) NPCs over multiple cell cycles.

(2) The affinity-purified complexes closely match known Nup84-associated proteins, indicating specificity and supporting utility for proteomics.

Weakness:

Reliance on GAL induction introduces metabolic shifts (raffinose → galactose → glucose) that could subtly alter cell physiology or the kinetics of NPC assembly. As acknowledged by the authors, alternative induction systems (e.g., β-estradiol-responsive GAL4-ER-VP16) could be implemented as a way to avoid carbon-source changes.

Comments on revised version.

The authors have thoughtfully addressed all of my concerns. In particular, they have updated the proteomic analysis in Figure 1I, showing that they recover most NPC components (including basket Nups), including non-NPC proteins as controls, and providing all data as a supplementary table. These changes strengthen the authors conclusion and improve transparency. I have no further recommendations and congratulate the authors for their exciting work.

https://doi.org/10.7554/eLife.108399.2.sa3

Reviewer #2 (Public review):

Summary:

This preprint describes a practical and useful approach for labeling and tracking NPCs in situ, using a fluorescently conjugated nanobody that binds directly to the core scaffold nucleoporin Nup84 with nanomolar affinity. Useful applications including timelapse imaging, affinity purification, and proximity labeling are envisioned.

Strengths:

Clever use of a fluorescently conjugated nanobody that binds directly to the core scaffold nucleoporin Nup84 with nanomolar affinity.

https://doi.org/10.7554/eLife.108399.2.sa2

Reviewer #3 (Public review):

Summary:

Submitted to the Tools and Resources series, this study reports on the use of a single-domain antibody targeting the nucleoporin Nup84 to probe and track NPCs in budding yeast. The authors demonstrate their ability to rapidly label or pull down NPCs by inducing the expression of a tagged version of the nanobody (Fig. 1).

Strengths:

This tool's main strength is its versatility as an inexpensive, easy-to-set-up alternative to metabolic labelling or optical switching. This same rationale could, in principle, be applied to the study of other multiprotein complexes using similar strategies, provided that single-chain antibodies are available.

Weaknesses:

This approach has no inherent weaknesses, but it would be useful to verify in the future that this pulse labelling strategy can also be used to detect assembly intermediates, structural variants, or damaged NPCs, e.g. NPC clusters formed in some nucleoporin mutants.

Overall, the data clearly shows that Nup84 nanobodies are a valuable tool for imaging NPC dynamics and investigating their interactomes through affinity purification.

Comments on revised version.

None at this stage.

https://doi.org/10.7554/eLife.108399.2.sa1

Author response:

The following is the authors' response to the original reviews.

> ***Public Reviews:***
>
> ***Reviewer #1 (Public review):***
>
> *Summary:*
>
> *The authors present a nanobody-based pulse-labeling system to track yeast NPCs. Transient expression of a nanobody targeting Nup84 (fused to NeonGreen or an affinity tag) permits selective visualization and biochemical capture of NPCs. Short induction effectively labels NPCs, and the resulting purifications match those from conventional Nup84 tagging. Crucially, when induction is repressed, dilution of the labeled pool through successive cell cycles allows the visualization of "old" NPCs (and potentially individual NPCs), providing a powerful view of NPC lifespan and turnover without permanently modifying a core scaffold protein.*
>
> *Strengths:*
>
> *(1) A brief expression pulse labels NPCs, and subsequent repression allows dilution-based tracking of older (and possibly single) NPCs over multiple cell cycles.*
>
> *(2) The affinity-purified complexes closely match known Nup84-associated proteins, indicating specificity and supporting utility for proteomics.*

We thank the reviewer for this evaluation

> *Weaknesses:*
>
> *(1) Reliance on GAL induction introduces metabolic shifts (raffinose -> galactose -> glucose) that could subtly alter cell physiology or the kinetics of NPC assembly. Alternative induction systems (e.g., β-estradiol-responsive GAL4-ER-VP16) could be discussed as a way to avoid carbon-source changes.*

Indeed, this could be an improvement, and we mention the benefits of an inducible system that does not alter the cell's metabolic state in the discussion on p.3.

> *(2) While proteomics is solid, a comprehensive supplementary table listing all identified proteins (with enrichment and statistics) would enhance transparency.*

Indeed, we now provide source data showing LFQ intensities, fold-enrichment and statistics for all detected proteins.

> *(3) Importantly, the authors note that the method is particularly useful "in conditions where direct tagging of Nup84 interferes with its function, while sub-stoichiometric nanobody binding does not." After this sentence, it would be valuable to add concrete examples, such as experiments examining NPC integrity in aging or stress conditions where epitope tags can exacerbate phenotypes. These examples will help readers identify situations in which this approach offers clear advantages.*

Indeed, we agree this would be useful. For example, in Nup1Δct and Nup60Δ mutants, GFP-tagging of Nup84 leads to slower growth and increased cell size (Ollivaud et al., BioRxiv). We have however not extensively tested nanobody expression in these mutants, and cannot conclude that it has no interfering effects. We therefore rephrased to "while sub-stoichiometric nanobody binding does may not, …". Another situation where we find the nanobody-based labeling useful is when we want to assess the structural integrity (IPs) and localization (imaging) of NPCs in mutant strains, but prefer not to use tagged Nups in the actual experiments. In these cases, we transiently express the Nup84 nanobody to perform these checks, and then carry out the experiments without the nanobody to avoid any tag-related interference. We hence also added ",…or when the temporary introduction of a ZZ- or mNG-tagged nanobody allows assessment of the integrity or localization of mutant NPCs prior to performing experiments without the nanobody.

We thank the reviewer again for the constructive feedback and thoughts.

> ***Reviewer #2 (Public review):***
>
> *Summary:*
>
> *This preprint describes a practical and useful approach for labeling and tracking NPCs in situ. While useful applications including timelapse imaging, affinity purification, or proximity labeling are envisioned, addressing some outstanding technical questions would give a clearer picture of the sensitivity and temporal resolution of this approach.*
>
> *Strengths:*
>
> *Clever use of a fluorescently conjugated nanobody that binds directly to the core scaffold nucleoporin Nup84 with nanomolar affinity.*

We thank the reviewer for this evaluation

> *Weaknesses:*
>
> *The decrease in nanobody labeling over 8 hours of chase period is interpreted to indicate that NPCs turn over during this time. However, it is also possible that the nanobody: Nup84 association is disrupted during mitosis by phosphorylation, other PTMs, or structural remodeling.*

We thank the reviewer for this thought. It is actually not turnover that we propose to underly the decrease in nanobody labeling, but rather the dilution of labelled NPC to the daughter cell. The current data do not support the interpretation that the nanobody: Nup84 association is disrupted as proposed by the reviewer. The exchange of individual Nups, including Nup84, is slow with half-times in the order of hours (Hakhverdyan et al. 2021; Rabut, Doye, and Ellenberg 2004), and the nanobody: Nup84 association is very stable, namely in the nanomolar range (Nordeen et al. 2020). The association of nanobody with NPCs is thus expected to be very stable. Instead, dilution of labelled NPCs to the daughter - approximately 40% of the existing NPCs are transmitted to the daughter cell in each division (Zsok et al. 2024; Khmelinskii et al. 2010) – will lead to significant decreases in nanobody labelling over time. As the reviewer is likely aware, baker's yeast NPCs – in contrast to mammalian NPCs - remain largely intact during cell division as there is no nuclear envelope breakdown.

We thank the reviewer again for the constructive feedback and thoughts.

> ***Reviewer #3 (Public review):***
>
> *Summary:*

> *Submitted to the Tools and Resources series, this study reports on the use of a single-domain antibody targeting the nucleoporin Nup84 to probe and track NPCs in budding yeast. The authors demonstrate their ability to rapidly label or pull down NPCs by inducing the expression of a tagged version of the nanobody (Figure 1).*
>
> *Strengths:*
>
> *This tool's main strength is its versatility as an inexpensive, easy-to-set-up alternative to metabolic labelling or optical switching. This same rationale could, in principle, be applied to the study of other multiprotein complexes using similar strategies, provided that single-chain antibodies are available.*

We thank the reviewer for this evaluation

> *Weaknesses:*
>
> *This approach has no inherent weaknesses, but it would be useful for the authors to verify that their pulse labelling strategy can also be used to detect assembly intermediates, structural variants, or damaged NPCs.*

We agree with the reviewer that it would be informative to see if VHH[Nup84] can bind its epitope in the context of an altered NPC structure but consider such studies to be beyond the scope of this study.

> *Overall, the data clearly show that Nup84 nanobodies are a valuable tool for imaging NPC dynamics and investigating their interactomes through affinity purification.*

We thank the reviewer again for the constructive feedback and thoughts.

> ***Recommendations for the authors:***
>
> ***Reviewer #1 (Recommendations for the authors):***
>
> *(1) In Figure 1A, and although it is partially mentioned in the legend, it would be helpful to indicate precisely when cells are grown in raffinose, when galactose is added for induction, and when glucose is used to terminate expression.*

We included “galactose” and “glucose” to Panel A to indicate induction and termination of expression, respectively.

> *(2) Related to the previous point, consider mentioning the GAL4-ER-VP16 (ADGEV) estradiol-inducible system as an optional strategy to avoid carbon shifts and potentially reduce cell-to-cell variability.*

We mention the benefits of an inducible system that does not alter the cell’s metabolic state in the discussion on p.3

> *(3) Add a brief sentence explaining that the ZZ tag is derived from Protein A and binds IgG Fc.*

This information is now added on p.2

> *(4) The statement "all Nups significantly coenriched with VHH[Nup84]-ZZ..." is likely inaccurate, since not all Nups are labeled in panels F-H, and some basket components are missing in panel I (particularly basket components such as Nup60, Nup1). Consider revising to "most Nups significantly coenriched...". In panel I, please include a clearly non-enriched protein as a visual reference for the color scale.*

We are very grateful to the reviewer for pointing this out. We accidentally used a faulty filtering on the dataset to generate figure panel I, omitting several Nups that were reproducibly found in all replicas. All Nups, except for Gle1 and Pom33, were detected reproducibly.

We have made the following adjustments to the figure panel and accompanying text:

In Fig. 1I, we included the missing Nups and 5 proteins that co-purified with VHH[Nup84] but not specifically enriched, as the reviewer suggested. They cluster in a separate group and their abundance is not going up in time. We randomly selected these 5 proteins from the list of genes that were reproducibly found in all four timepoints.

For clarity, we removed the NTRs

We changed the text to “we found that all Nups, except Gle1 and Pom33, significantly coenriched with VHH[Nup84]-ZZ” on p.2.

We updated the methods section, describing the clustering method and how we selected the 5 random proteins

> *(5) Provide a supplementary spreadsheet with LFQ intensities, fold-enrichment, and statistics for all detected proteins. This will address questions about missing Nups and support transparency.*

This information is now added as Source data Figure 1.

> *(6) Directly after the statement "Amongst others this is useful in conditions where direct tagging of Nup84 interferes with its function, while sub stoichiometric nanobody binding does not," it would be useful to include concrete instances, such as stress or aging conditions, where Nup84 tagging may sensitize NPC integrity.*

Indeed, we agree this would be useful. For example, in Nup1Δct and Nup60Δ mutants, GFP-tagging of Nup84 leads to slower growth and increased cell size (Ollivaud et al., BioRxiv). We have however not extensively tested nanobody expression in these mutants and cannot conclude that it has no interfering effects. We therefore rephrased to “while sub-stoichiometric nanobody binding does may not, …”. Another situation where we find the nanobody-based labeling useful is when we want to assess the structural integrity (IPs) and localization (imaging) of NPCs in mutant strains, but prefer not to use tagged Nups in the actual experiments. In these cases, we transiently express the Nup84 nanobody to perform these checks and then carry out the experiments without the nanobody to avoid any tag-related interference. We hence also added “,…or when the temporary introduction of a ZZ- or mNG-tagged nanobody allows assessment of the integrity or localization of mutant NPCs prior to performing experiments without the nanobody.

> *(7) In panels K and L, since individual points correspond to biological replicates, overlaying a box plot obscures much of the data. Consider overlaying the means per replicate instead of box plots: see the "SuperPlots" approach for a clear explanation of how to present this (PMID: 32346721).*

We thank the reviewer for the “SuperPlots” suggestion, and we agree that representing the data in this way improves the visualization of individual biological replicates. We have updated the summarizing overlay in figures in panel K and L to represent the means per replicate instead of boxplots.

> *(8) I spotted a few typos ("Lasty" ? "Lastly"; "in maintained" vs. "is maintained").*

Thank you, these are corrected

> *Overall, this is a neat, well-executed methodological advance with clear value to the NPC field and potentially other complex assemblies. I look forward to seeing a revised version.*

Thank you!

> ***Reviewer #2 (Recommendations for the authors):***
>
> *Based on the recent structural analyses and NPC modeling using this nanobody, how accessible is the Nup84 epitope expected to be within the fully assembled NPC? While the data shown indicate that nanobody labeling of NPCs is readily detectable, stating this clearly would help motivate the approach and interpret the resulting data.*

We now included such a statement in the introduction on p.1.

> *The decrease of nanobody labeling over 8 hours of chase period is interpreted to indicate that NPCs turn over due to cell division during this time window. However, it is also possible that nanobody:Nup84 association is disrupted during mitosis by phosphorylation, other PTMs, or structural remodeling.*

We thank the reviewer for this thought. It is actually not turnover that we propose to underly the decrease in nanobody labeling, but rather the dilution of labelled NPC to the daughter cell. The current data do not support the interpretation that the nanobody: Nup84 association is disrupted as proposed by the reviewer. The exchange of individual Nups, including Nup84, is slow with half-times in the order of hours (Hakhverdyan et al. 2021; Rabut, Doye, and Ellenberg 2004), and the nanobody: Nup84 association is very stable, namely in the nanomolar range (Nordeen et al. 2020). The association of nanobody with NPCs is thus expected to be very stable. Instead, dilution of labelled NPCs to the daughter - approximately 40% of the existing NPCs are transmitted to the daughter cell in each division (Zsok et al. 2024; Khmelinskii et al. 2010) – will lead to significant decreases in nanobody labelling over time. As the reviewer is likely aware, baker's yeast NPCs – in contrast to mammalian NPCs - remain largely intact during cell division as there is no nuclear envelope breakdown.

> ***Reviewer #3 (Recommendations for the authors):***
>
> *(1) As mentioned above, to assess the general relevance of this tool, it would be informative to verify whether the VHH[Nup84] nanobody can access and detect NPC species under conditions that challenge their structural organization or biogenesis, for example, in nucleoporin mutants or under stress. The authors could, for instance, analyze the localization of VHH[Nup84] in yeast strains harboring clustered NPCs (nup133Δ), or following stresses known to impact NPC organization (e.g., osmotic stress or energy depletion; PMID: 34762489).*

We agree with the reviewer that it would be informative to see if VHH[Nup84] can bind its epitope in the context of an altered NPC structure and tried to include such data. Unfortunately, this was not successful, and further efforts are beyond the scope of his study. Following the reviewer's suggestion, we expressed VHH[Nup84] in *nup*133ΔN (nup133Δ2-300) (Doye, Wepf, and Hurt 1994) following the experimental set-up in panel A and examined its localization. However, at t=2hrs hardly any nanobody signal was detectable in *nup133ΔN* (see Author response image 1, upper panel A) and only after overnight expression nanobody-labelled NPC clusters are detectable (bottom panel A). Considering that expression levels of free mNG are also lower at t=2hrs in *nup133ΔN* cells compared to WT cells (Author response image 1, panel B), it appears that protein expression under the Gal system is generally reduced in a *nup133ΔN* background. These expression level differences between *nup133ΔN* and WT preclude statements about the accessibility of the Nup84 epitope in *nup133ΔN*. We note that nup133ΔN cells do not have general mRNA export defects (Doye, Wepf, and Hurt 1994), so other inducible systems may be better suited for such analysis.

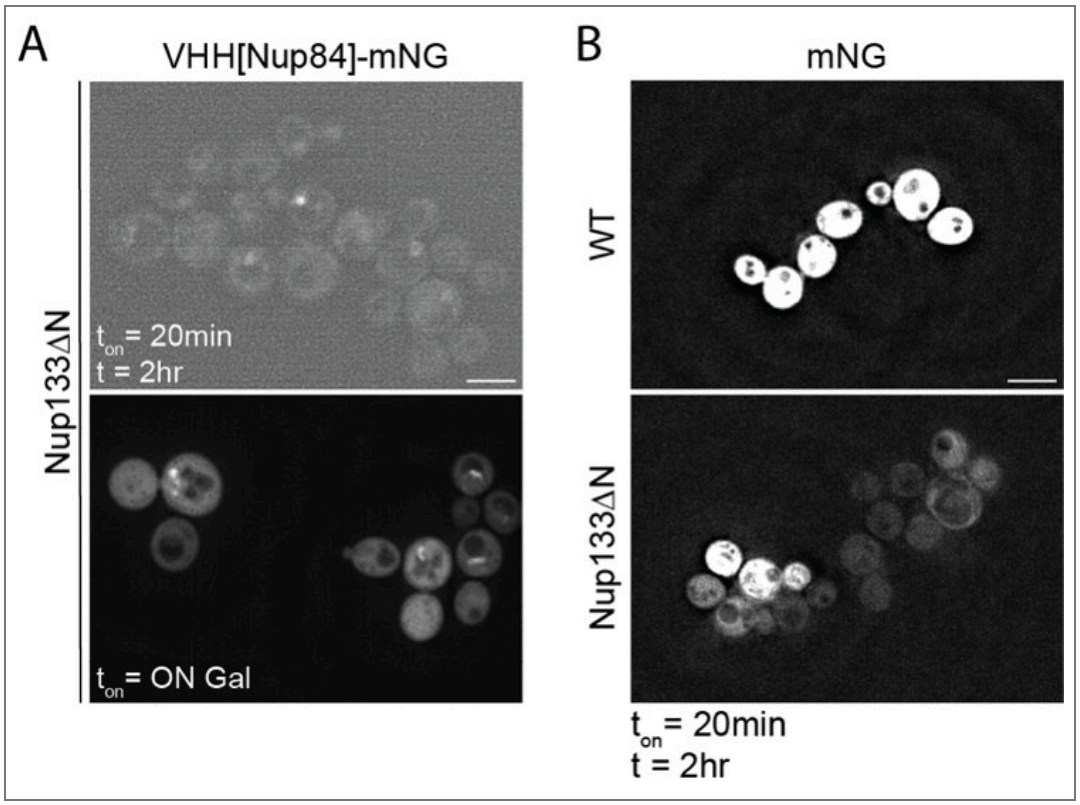

Author response image 1. Expression level differences in WT and Nup133ΔN cells. Left: localization of VHH[Nup84]-mNG in Nup133ΔN cells at t=2hr following a 20-minute induction pulse and after overnight 0.5% galactose (ON) induction. Right: mNG levels in WT and Nup133ΔN cells at t=2hr following a 20-minute induction pulse. Brightness/contrast settings are identical between the two panels. All panels are sum slices projections from 30 z-slices of 0.1µm. Scale bar = 5 µm.

> *(2) Since outer rings are found on both sides of NPCs (i.e., the cytoplasmic and nuclear faces), could the authors indicate whether the VHH[Nup84] nanobody can enter the nucleus and probe the nuclear outer rings? Along these lines, it would be useful to provide a summary of the structural organization of NPCs in the introduction.*

Thank you, we have added a sentence on the localization of Nup84 in NPCs in the introduction. Based on what is known about influx (nuclear transport receptor-independent nuclear entry) of proteins with similar size and surface properties (Popken et al. 2015; Timney et al. 2016), the nanobody can rapidly enter the nucleus and hence bind Nup84 on both the nuclear and cytoplasmic side. We have no data to answer if binding might initially be biased towards cytosolic VHH[Nup84] binding the cytoplasmic outer rings.

> *(3) The authors state that VHH[Nup84] and direct Nup84 detection are indistinguishable (p. 2). Could they provide images of the endogenously tagged Nup84-GFP strain for comparison?*

We have now included a pairwise comparison in a Figure 1 – supplement 1.

> *Minor corrections:*
>
> *(1) There are a few typos that need correcting: 'Nup84Δ' (p. 1; should read 'nup84Δ') and 'promotor' (p. 2; should read 'promoter').*

Thank you, these are corrected

> *(2) The reference 'Veldsink et al. 2025' (quoted in the PunctaFinder analysis description on page 8) does not appear in the References section.*

Thank you, these are corrected.

We thank the reviewer again for the constructive feedback and thoughts.

References

Doye, V., R. Wepf, and E. C. Hurt. 1994. 'A novel nuclear pore protein Nup133p with distinct roles in poly(A)+ RNA transport and nuclear pore distribution', EMBO J, 13: 6062-75.

Khmelinskii, Anton, Philipp J. Keller, Holger Lorenz, Elmar Schiebel, and Michael Knop. 2010. 'Segregation of yeast nuclear pores', Nature, 466: E1-E1.

Popken, Petra, Ali Ghavami, Patrick R. Onck, Bert Poolman, and Liesbeth M. Veenhoff. 2015. 'Size-dependent leak of soluble and membrane proteins through the yeast nuclear pore complex', Molecular Biology of the Cell, 26: 1386-94.

Timney, Benjamin L., Barak Raveh, Roxana Mironska, Jill M. Trivedi, Seung Joong Kim, Daniel Russel, Susan R. Wente, Andrej Sali, and Michael P. Rout. 2016. 'Simple rules for passive diffusion through the nuclear pore complex', Journal of Cell Biology, 215: 57-76.

Zsok, J., F. Simon, G. Bayrak, L. Isaki, N. Kerff, Y. Kicheva, A. Wolstenholme, L. E. Weiss, and E. Dultz. 2024. 'Nuclear basket proteins regulate the distribution and mobility of nuclear pore complexes in budding yeast', Mol Biol Cell, 35: ar143.

https://doi.org/10.7554/eLife.108399.2.sa0